

# All-electrical control of single ion spins in a semiconductor

Jian-Ming Tang,<sup>1</sup> Jeremy Levy,<sup>2</sup> and Michael E. Flatté<sup>1</sup>

<sup>1</sup>Department of Physics and Astronomy, University of Iowa, Iowa City, IA 52242-1479

<sup>2</sup>Department of Physics and Astronomy, University of Pittsburgh, Pittsburgh, Pennsylvania 15260, USA

We propose a method for all-electrical initialization, control and readout of the spin of single ions substituted into a semiconductor. Mn ions in GaAs form a natural example. In the ion's ground state the Mn core spin magnetic moment locks antiparallel to the spin and orbital magnetic moment of a bound valence hole from the GaAs host. Direct electrical manipulation of the ion spin is possible because electric fields manipulate the orbital wave function of the hole, and through the spin-orbit coupling the spin is reoriented as well. Coupling two or more ion spins can be achieved using electrical gates to control the size of the valence hole wave function near the semiconductor surface. This proposal for coherent manipulation of individual ionic spins and controlled coupling of ionic spins via electrical gates alone may find applications in extremely high density information storage and in scalable coherent or quantum information processing.

PACS numbers: 73.20.-r, 76.30.Da, 03.67.Lx, 75.75.+a

Observing magnetic resonance between different spin states of nuclei or electrons is a technique widely used in many imaging and spectroscopic applications. Sensitivity sufficient to measure the fluctuation of a single spin has been demonstrated using magnetic resonance force microscopy [1], noise spectroscopy [2], optical spectroscopy [3, 4], scanning tunneling microscopy (STM) [5, 6, 7], and quantum point contact conductivity [8]. The potential also exists to determine the spin state [2, 4, 8, 9]. Controlling a single spin, in addition to monitoring it, is highly desirable for building future spin-based devices, is essential for quantum computation, and should permit the direct exploration of fundamental aspects of quantum dynamics in a solid state environment [10, 11, 12, 13]. Proposed schemes to control a single spin in a solid state environment rely either on magnetic resonance [14, 15] or optical manipulation [16, 17, 18], and there has been progress towards replacing magnetic control fields with the spin-orbit interaction [19, 20] or the exchange interaction [21, 22].

Ionic spin states in solids have several attractive characteristics for fundamental studies of spin dynamics and for spin-based devices. Every ion embedded in a solid is identical to every other such ion, as are their electronic spin states. Thus an ionic spin system can be as uniform as a nuclear spin system, but also can permit spin manipulation on short time scales as in a quantum dot spin system. Initializing, controlling and detecting ionic single spins without any magnetic fields, using techniques in which electric fields play the typical role of magnetic fields, may therefore provide a path to high-density scalable spin-based electronics. For example, the control of ionic spin states can be used to produce highly spin-selective and spin-dependent tunneling currents in nanoscale electrical devices, or to realize quantum computation. Furthermore the manipulation of individual spins that are constituents of interacting spin clusters opens up the capability to explore the fundamental dy-

namics of frustrated spin systems and other correlated spin systems.

Here we propose an all-electrical scheme for ionic spin manipulation in which the role of magnetic fields in traditional electron spin resonance (ESR) is replaced by electric fields. In conventional ESR the energy splitting between different spin states, and the couplings between them, are controlled by magnetic fields because an electric field does not directly couple to the electron's spin. In a semiconductor crystal with tetrahedral symmetry and spin-orbit interaction (such as GaAs) a  $J = 1$  ion spin (such as that of Mn) will be triply degenerate, however the energy splittings and the couplings between these states depend linearly on the electric field strength, allowing rapid all-electrical control. Thus initialization, manipulation, and detection, operations performed with magnetic fields in traditional ESR, can be performed with all-electrical techniques.

A specific proposed setup for manipulating a single spin is shown in Fig. 1. Tip-induced placement of single Mn ions in a conductive GaAs sample has been demonstrated experimentally [23]. The sample has two gates configured to apply an electric field along the [001] direction, with the Mn ion substituted for a Ga as the single spin. A third connection, which will be used as a gate for spin manipulation, and as a contact for initialization and detection, is an STM tip. The surface normal is parallel to the [110] direction, taking advantage of a natural cleavage plane of GaAs that lacks surface states. The applied electric field is confined in the plane defined by these two axes and is specified by the angle from the [001] axis.

A neutral Mn dopant in GaAs forms a single compound spin with total angular momentum  $J = 1$ . An isolated Mn ion has a half-filled 3d shell and the spins of all five electrons in the 3d shell are aligned as a result of the exchange interaction (Hund's rule) to form a  $S = 5/2$  ground state. When put in a tetrahedral semiconductor

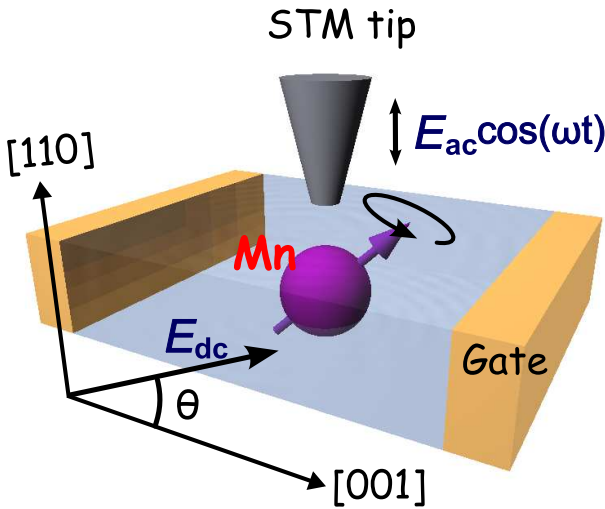


FIG. 1: (color online) Proposed configuration for the electric resonances of a single Mn dopant in GaAs. A dc electric field  $E_{dc}$  is applied via the electrical gates and the STM tip. The resonance is driven by an additional small ac field.

the Mn substitutes for a Ga ion, and a hole in the valence band is created to compensate for the differing valences of Mn and Ga. We describe the core spin-valence hole dynamics with the following effective spin Hamiltonian:

$$H_{\text{spin}} = S \cdot s + l \cdot s;$$

where  $l$  and  $s$  are the orbital angular momentum and the spin of the bound hole respectively. Our tight-binding calculations [24] estimate the exchange coupling and the spin-orbit coupling for this bound hole wavefunction to be about 300 meV and 80 meV respectively. Thus the exchange interaction binds the valence hole with antiparallel spin to the  $S = 5/2$  Mn core spin with a binding energy of 113 meV [25], and orients the hole's angular momentum antiparallel to the Mn core spin. The second term in Eq. (1) comes from the spin-orbit interaction in GaAs, and configures the valence hole spin ( $s = 1/2$ ) parallel to its orbital angular momentum ( $l = 1$ ). The total angular momentum of the (Mn core + hole) complex is  $J = S + l + s$ , and the ground state of the Mn complex will have total angular momentum  $J = 1$  [26]. The triply-degenerate  $J = 1$  character of the ground state of this embedded ion has been confirmed via ESR [26]. Our proposals for spin control will involve energy scales smaller than  $E_{dc}$ , so for the purposes of this paper only the lowest energy multiplet with  $J = 1$  is of interest (both  $l$  and  $s$  are antiparallel to  $S$ ).

The degeneracy of the  $J = 1$  Mn ion can be substantially split by external electric fields, and the eigenstates

depend strongly on the electric field direction. This will be the source both of state splitting (analogous to the static magnetic field in traditional ESR) and state coupling (analogous to the oscillating perpendicular magnetic field in traditional ESR). We find the following electric-field-dependent Hamiltonian:

$$H_I(E) = E_x (J_y J_z + J_z J_y) + c.p. ; \quad (2)$$

where  $E$  is an electric field,  $c.p.$  stands for cyclic permutation, and  $x, y, z$  stand for the 3 major axes of the cubic crystal. Note that this Hamiltonian does not break time-reversal symmetry for the angular momentum operators  $J$  always appear in pairs. We calculate, using the probability densities of the hole state found in our tight-binding calculations and first-order perturbation theory,

$= 6.4 \cdot 10^{30} \text{ C m}$ , corresponding to  $E = 160 \text{ eV}$  for  $E = 40 \text{ kV/cm}$ . This exceptionally large splitting is equivalent to that generated by applying a 1 Tesla magnetic field using the measured g-factor [26], 2.77. The linear dependence on electric field, critical to producing a large splitting, originates from the lack of inversion symmetry of the substituted ion in a tetrahedral host. The energy splittings from an electric field applied to bound states at inversion-symmetric sites in crystals, or electrons bound in atoms or ions in vacuum, would depend quadratically on the electric field and would be correspondingly much smaller. The other essential element causing this large splitting is the large ( $10 \text{ \AA}$ ) Bohr radius of the bound valence hole [24, 27]. Recent progress in theory and scanning tunneling microscopy of Mn dopants in III-V semiconductors has confirmed the large spatial extent of the bound hole wavefunction [23, 24, 27, 28]. Thus the response of the Mn wavefunction to electric fields is substantial compared to other ion levels associated with transition-metal (magnetic) dopants.

In the basis  $|x\rangle, |y\rangle$  and  $|z\rangle$  for Eq. (2), in which  $J_z = 0$ , the interaction Hamiltonian is

$$H_I(E) = \begin{pmatrix} 0 & 0 & 1 \\ 0 & \hat{E}_z & \hat{E}_y \\ 0 & \hat{E}_y & \hat{E}_x \end{pmatrix} : \quad (3)$$

The energy eigenvalues in units of  $E$  are the roots of the characteristic polynomial,

$$x^3 - x + 2 = 0 ; \quad (4)$$

where  $= \hat{E}_x \hat{E}_y \hat{E}_z$ . A static electric field  $E_{dc}$  splits all three eigenstates in energy except when the field is in the [111] direction, for which  $= 1$  and two of the eigenstates remain degenerate. For  $= 0$ , the three split levels are equally spaced.

The energies of the three states are  $1 = (\cos \frac{\pi}{4} - 3\cos^2 \frac{\pi}{4})^{1/2} = 2$ ,  $2 = (\cos \frac{\pi}{4} + 3\cos^2 \frac{\pi}{4})^{1/2} = 2$ , and  $3 = \cos \frac{\pi}{4}$ , shown by the solid, dashed, and dotted curves respectively in Fig. 2(a). The eigenstate  $|z\rangle$  is

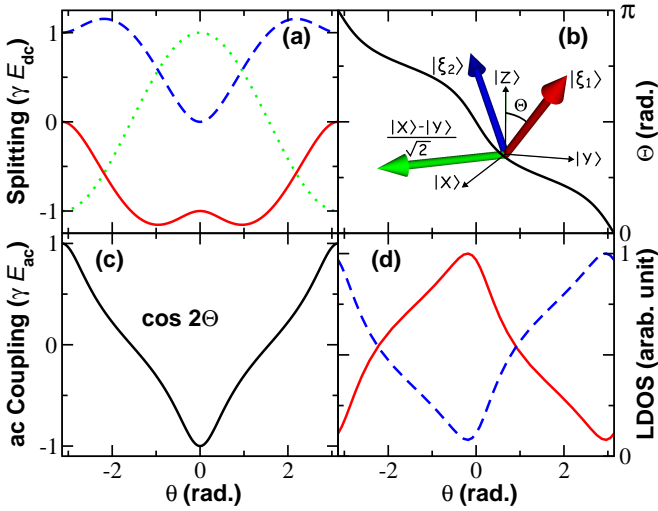


FIG. 2: (color online) The ionic spin system as a function of the dc field orientation. (a) The energies of the  $J = 1$  states  $|j_{1i}\rangle$  (solid),  $|j_{2i}\rangle$  (dashed), and  $|j_{3i}\rangle$  (dotted). (b) The corresponding eigenvectors parametrized by the angle  $\theta$ . (c) The coupling between  $|j_{1i}\rangle$  and  $|j_{2i}\rangle$  due to the ac field. (d) The scaled LDOS of the two possible final states  $|j_{1i}\rangle$  (solid) and  $|j_{2i}\rangle$  (dashed) probed four monolayers directly above the Mn dopant.

$|j_{1i}\rangle$  is independent of the electric field orientation. The independence of  $|j_{3i}\rangle$  from  $E$  motivates us to define a pseudospin  $1/2$  constructed from the other two states,  $|j_{1i}\rangle$  and  $|j_{2i}\rangle$ . These eigenstates can be written in terms of a single parameter as  $|j_{1p}\rangle = (\sin \theta; \sin \theta; 2 \cos \theta)$  and  $|j_{2p}\rangle = (\cos \theta; \cos \theta; 2 \sin \theta)$ , where  $\theta$  is the angle of between  $|j_{1i}\rangle$  and the  $|z\rangle$  basis (Fig. 2(b)). Note that all the eigenvectors are real because of time-reversal symmetry.

Preparation of the initial pseudospin state is achieved by applying an electric field to split the state energies, and allowing the hole to relax into the ground state. The electric field from the STM tip locally bends the bands of the semiconductor and permits ionization of the bound hole; this has been demonstrated for Mn in GaAs [27, 29]. Rapid initialization of a high purity pseudospin state can be achieved by using the local band bending effect to move the two higher-energy levels ( $|j_{2i}\rangle$ ,  $|j_{3i}\rangle$ ) to the position shown in Fig. 3(a), so a hole in those states would ionize and be replaced by a hole in the lowest energy state ( $|j_{1i}\rangle$ ). At a temperature of 0.5 K and a dc field of 100 kV/cm, the occupation of the next highest state ( $|j_{2i}\rangle$ ) would be less than  $10^{-4}$ . We have chosen  $E_{dc}$  such that  $(-\tan^{-1} \frac{1}{2}) < \theta < (\tan^{-1} \frac{1}{2})$ , so that  $|j_{1i}\rangle$  (not  $|j_{3i}\rangle$ ) is the ground state (see Fig. 2(a)). Band bending also changes the effective radius of the bound hole wave function; gate voltages applied at the surface could thus control the coupling of two bound hole states in an analogous way to approaches in Refs. 14, 15 for quantum dots and donor states.

In order to manipulate the initialized spins the tip-

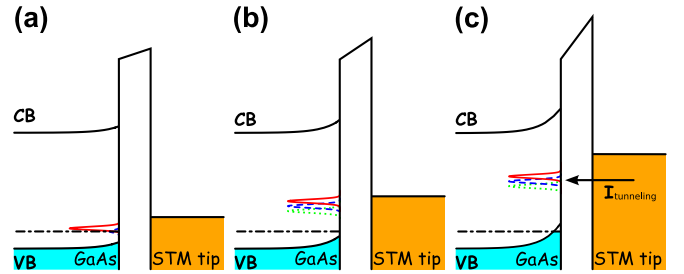


FIG. 3: (color online) Schematics of controlling the spin states via local band bending. The dot-dashed lines show the chemical potential. Shaded regions are filled states. CB and VB label the conduction and valence bands of the semiconductor. (a) Initialization: The height of each peak represents the occupation probability of holes in that state. For this voltage occupation of the  $|j_{1i}\rangle$  state dominates. (b) Manipulation: Bring all the states into the gap, but control the bias voltage below the threshold where the current starts to tunnel through these states. The oscillating field ( $E_{ac}$ ) drives transitions between the  $|j_{1i}\rangle$  and the  $|j_{2i}\rangle$  states. (c) Detection: Bring the final state further into the gap, so that electrons can tunnel from the tip into the acceptor state. The final state is identified according to the amplitude of the tunneling current (Fig. 2(d)).

sample bias should be increased adiabatically (slower than  $h = (E_{dc})$ ) to bring all three levels into the semiconductor's energy gap (see Fig. 3(b)). This shift with bias is described for Mn in p-doped GaAs in Ref. [27]. The bias voltage has to be maintained below the critical value at which electrons start to tunnel directly through these levels, so that the transitions between these states remain coherent. Spin resonance can now be driven by applying a small oscillating electric field  $E_{ac}(t)$  to the static field  $E_{dc}$ . The Hamiltonian

$$H_{\text{ESR}} = H_I(E_{dc}) + H_I(E_{ac}(t)): \quad (5)$$

To have a well-defined pseudospin  $1/2$ , constructed out of  $|j_{1i}\rangle$  and  $|j_{2i}\rangle$ , the coupling of these two states to  $|j_{3i}\rangle$  must vanish. For the schematic in Fig. 1 the oscillating field can be applied either along the  $[110]$  direction through the STM tip or along the  $[001]$  direction through the gates. Both choices leave  $|j_{3i}\rangle$  unaffected and only couple  $|j_{1i}\rangle$  and  $|j_{2i}\rangle$  to each other. To see how the states are coupled by the ac field, we write out  $H_I(E_{ac}(t))$  using the eigenstates of  $H_I(E_{dc})$  as bases. We assume that the ac field  $E_{ac}(t)$  is along the  $[110]$  direction.

$$H_I(E_{ac}(t)) = \begin{bmatrix} 0 & \sin 2\theta & \cos 2\theta & 0 \\ E_{ac} \cos(\omega t) & 0 & \cos 2\theta & \sin 2\theta \\ 0 & \cos 2\theta & 0 & 0 \\ 0 & 0 & 0 & 0 \end{bmatrix} \quad (6)$$

The off-diagonal term  $\cos 2\theta$ , plotted in Fig. 2(c), shows how the coupling between the two coupled states changes with the field orientation. The coupling is maximized when the static field is completely along the  $[001]$  direction ( $\theta = 0$ ). Then the static and oscillating electric fields

are perpendicular to each other, just as the static and oscillating magnetic fields are perpendicular to each other in traditional ESR. In the limit  $E_{ac} \gg E_{dc}$ , the diagonal term can be neglected and our configuration works just like conventional ESR. The Rabi frequency obtained from the standard Rabi formula is

$$\omega = \frac{1}{2} \frac{q}{(E_{ac} \cos^2 \theta)^2 + (h \frac{1}{E_{dc}} \frac{4}{\cos^2 \theta})^2} : \quad (7)$$

For  $E_{ac} = E_{dc} = 25 \text{ kV/cm}$ , and  $\theta = 2^\circ$ ,  $\omega = 12 \text{ GHz}$ , corresponding to a Rabi time of 80 ps. Ensemble spin coherence times  $T_2$  measured by traditional ESR in GaMnAs exceed 0.5 ns (several times the estimated Rabi time), and appear due to the inhomogeneous environments of Mn ions [26]; the  $T_2$ 's of individual spins are expected to be considerably longer. Hyperfine interactions, which significantly affect conduction electron spin coherence, are expected to be weak for Mn ions as the overlap of the valence p orbitals with the nucleus is small.

High-fidelity determination of the orientation of the pseudospin can be achieved by measuring the total tunneling current through the final state with the STM [9]. When the tip-sample voltage is increased, and the semiconductor bands bend further (see Fig. 3(c)), current starts to tunnel through the bound hole wavefunction state [27, 29] and the tunneling current is proportional to the probability density of the state at the STM tip location. The spatial structure of these  $J = 1$  states is highly anisotropic [24, 27, 29]. We calculate the two eigenstates to have the following spatial structure,

$$h_{Rj_1i} = c_{x,y}^i (h_{Rj_1} X + Y) + c_z^i h_{Rj_2i} ; \quad (8)$$

where  $c_{x,y}^1 = \sin \theta$  and  $c_{x,y}^2 = \cos \theta$ . If the STM tip is positioned directly over the Mn dopant, it probes the nodal plane,  $h_{Rj_2i} = 0$ . In this particular case, the LDOS is simply proportional to the projection on to the  $h_{Rj_1} X + Y$  state, which is  $j \sin \theta$  for  $j_1 i$ , and  $j \cos \theta$  for  $j_2 i$ . Thus for a static electric field along  $\theta = 0$  ( $\theta = 90^\circ$ ) and the pseudospin in the  $j_2 i$  state no current will be detected, but for the pseudospin in the  $j_1 i$  state there will be current detected. The difference in current for the  $j_1 i$  and  $j_2 i$  states is shown in Fig. 2(d). For this position about 10% of the LDOS is not spin dependent, which reduces maximum visibility to 90% (at, e.g.,  $\theta = 0$ ). Spatial averaging of the LDOS over a typical experimental 2 Å changes the visibility by only a few percent. The asymmetric angular dependence is due to the lack of inversion symmetry of the substituted ion in a tetrahedral host. Current measurement timescales can be very fast as STM experiments performed at 50 GHz have demonstrated [30]. We also assume that the tunneling current is small so that spin flip does not occur during the measurement.

Controllable coupling of two spins permits the use of these Mn ions for quantum information processing. Estimates

of the overlap of holes bound to two separated Mn ions [24] indicate 100 meV splittings of Mn pair states for ions separated by 12 Å along the (110) direction. The overlap falls off for larger separations according to the

13 Å wave function radius of the bound hole, so would be 0.1 meV for two ions 10 nm apart. This overlap could be reduced, increased, or eliminated with a gate between the two ions [14, 15]. By using single-Mn manipulations to put single-ion quantum information in the proper pair of single-Mn states, the Mn pair state splitting can be used to perform CNOT operations in an analogous way to how the singlet-triplet splitting is used for a CNOT with spin  $1/2$  qubits.

In conclusion, we have presented a concrete proposal for electrically initializing, manipulating, and detecting single pseudospin states of a magnetic dopant in a semiconductor. All-electrical spin manipulation should be possible for other impurities in tetrahedral semiconductors characterized by  $J > 1/2$  ground state spins (e.g. most transition metal ions in most tetrahedral semiconductors, or the nitrogen-vacancy center in diamond). In a future scalable architecture the STM tip would be replaced by a gate-controlled contact. The controlled resistance of that contact would permit alternation between the gate configuration for manipulation and the contact configuration for initialization and detection, without moving parts. The [001] static electric field, here assumed to be implemented with gates, may also be replaced by an internal electric field from a doping gradient (such as in a p-n junction), or even a static strain field. The Mn ions could be controllably placed within the surface relative to the contacts using current pulses from an STM tip as described in Ref. 23.

This work is supported by ARO MURI DAAD 19-01-1-0541 and DARPA QuIST DAAD-19-01-1-0650.

---

- [1] D. Rugar, R. Budakian, H. J. Mamin, and B. W. Chui, *Nature* 430, 329 (2004).
- [2] M. Xiao, I. Martin, E. Yablonovitch, and H. W. Jiang, *Nature* 430, 435 (2004).
- [3] A. Gubser, A. Dabre, C. Tietz, L. Fleury, J. Wachtrup, and C. von Borczyskowski, *Science* 276, 2012 (1997).
- [4] F. Jelezko, I. Popa, A. Gubser, C. Tietz, J. Wachtrup, A. Nizovtsev, and S. Kulin, *Appl. Phys. Lett.* 81, 2160 (2002).
- [5] Y. M. Manassen, R. J. Hammars, J. E. Demuth, and A. J. Castellano, Jr., *Phys. Rev. Lett.* 62, 2531 (1989).
- [6] C. Durkan and M. E. Wall, *Appl. Phys. Lett.* 80, 458 (2002).
- [7] A. J. Heinrich, J. A. Gupta, C. P. Lutz, and D. M. Eigler, *Science* 306, 466 (2004).
- [8] J. M. Elzerman, R. Hanson, L. H. W. van Beveren, B. Witkamp, L. M. K. Vandersypen, and L. P. Kouwenhoven, *Nature* 430, 431 (2004).

[9] J.-M. Tang and M. E. Flatté, *Phys. Rev. B* **72**, 161315(R) (2005).

[10] G. Prinz, *Science* **282**, 1660 (1998).

[11] S. A. Wolf, D. D. Awschalom, R. A. Buhrman, J. M. Daughton, S. von Molnar, M. L. Roukes, A. Y. Chtchelkanova, and D. M. Treger, *Science* **294**, 1488 (2001).

[12] M. Ziese and M. J. Thornton, eds., *Spin Electronics*, vol. 569 of *Lecture Notes in Physics* (Springer-Verlag, Berlin, 2001).

[13] D. D. Awschalom, N. Samarth, and D. Loss, eds., *Semiconductor Spintronics and Quantum Computation* (Springer-Verlag, Berlin, 2002).

[14] D. Loss and D. P. DiVincenzo, *Phys. Rev. A* **57**, 120 (1998).

[15] B. E. Kane, *Nature* **393**, 133 (1998).

[16] A. Imamoglu, D. D. Awschalom, G. Burkard, D. P. DiVincenzo, D. Loss, M. Sherwin, and A. Small, *Phys. Rev. Lett.* **83**, 4204 (1999).

[17] C. E. Pryor and M. E. Flatté, quant-ph/0211160 (2002).

[18] G. F. Quinteiro and C. Piemarcocchi, *Phys. Rev. B* **72**, 045334 (2005).

[19] Y. Kato, R. C. Myers, D. C. Driscoll, A. C. Gossard, J. Levy, and D. D. Awschalom, *Science* **299**, 1201 (2003).

[20] Y. K. Kato, R. C. Myers, A. C. Gossard, and D. D. Awschalom, *Nature* **427**, 50 (2004).

[21] D. P. DiVincenzo, D. Bacon, J. Kempe, G. Burkard, and K. B. Whaley, *Nature* **408**, 339 (2000).

[22] J. R. Petta, A. C. Johnson, J. M. Taylor, E. A. Laird, A. Yacoby, M. D. Lukin, C. M. Marcus, M. P. Hanson, and A. C. Gossard, *Science* **309**, 2180 (2005).

[23] D. K. Ritchie, A. R. Ichardella, and A. Yazdani, *J. of Superconductivity* **18**, 23 (2005).

[24] J.-M. Tang and M. E. Flatté, *Phys. Rev. Lett.* **92**, 047201 (2004).

[25] T. C. Lee and W. W. Anderson, *Solid State Commun.* **2**, 265 (1964).

[26] J. Schneider, U. Kauflmann, W. Wilkening, M. Baeumer, and F. Kohl, *Phys. Rev. Lett.* **59**, 240 (1987).

[27] A. M. Yakunin, A. Y. Silov, P. M. Koenraad, J. H. Wolter, W. Van Roy, J. De Boeck, J.-M. Tang, and M. E. Flatté, *Phys. Rev. Lett.* **92**, 216806 (2004).

[28] P. I. Arseev, N. S. Maslova, V. I. Panov, S. V. Savinov, and C. van Haesendonck, *Pis'ma Zh. Eksp. Teor. Fiz.* **77**, 202 (2003), [*JETP Lett.* **77**, 172 (2003)].

[29] A. M. Yakunin, A. Y. Silov, P. M. Koenraad, W. Van Roy, J. De Boeck, and J. H. Wolter, *Physica E* **21**, 947 (2004).

[30] G. M. Steeves, A. Y. Elzababi, and M. R. Freeman, *Appl. Phys. Lett.* **72**, 504 (1998).